Supporting Information

Dual-mode avocado-like all-iron nanoplatform for enhanced T_1/T_2 MRI-guided tumor therapy

Jing Li[a], Xincong Li[a], Siman Gong[a], Cuiting Zhang [a], Chenggen Qian[a], Hongzhi Qiao[b], Minjie Sun[a],*

[a]State Key Laboratory of Natural Medicines, Department of Pharmaceutics, China Pharmaceutical University, 24 Tong Jia Xiang, Nanjing 210009, China

[b]School of Pharmacy, Nanjing University of Chinese Medicine, Nanjing 210023, China

*Email: msun@cpu.edu.cn

Experimental section

Materials

Dopamine hydrochloride, PVP-K30 and tannic acid were purchased from Aladdin Reagent Database Inc. (Shanghai, China). Iron chloride hexahydrate ($FeCl_3 \cdot 6H_2O$) was provided by Sinopharm Chemical Reagent Co., Ltd. (Shanghai, China). Doxorubicin hydrochloride (DOX) was bought from Shenzhen Main Luck Pharmaceuticals Inc. (Shenzhen, China). γ-Fe_2O_3 nanoparticle is a kind gift from Professor Ning Gu of Southeast University. 3-(4, 5-Dimethylthiazol-2-yl)-2, 5-diphenyl-tetrazolium bromide (MTT), Calcein-AM/PI double staining kits and cell culture materials, including RPMI 1640, DMEM (high glucose) were provided by Kaiji Biotechnology (Nanjing, China).

Preparation and characterization of CNMN

Before the fabrication of CNMN nanoplatform, Fe_2O_3@ PDA was synthesized according to the previous reports.[1] Then the $FeCl_3 \cdot 6H_2O$ (0.5 ml, 20mg/ml) and TA solution (0.5ml, 40mg/ml) was dropped into Fe_2O_3@ PDA (3 ml, 2 mg/ml) solution, and the mixture pH was adjusted to 5.5. After being stirred 4h under room temperature, the obtained nanoplatform was purified by centrifugation and washed with water for three times. Subsequently 10 mg PVP-K30 was added to the nanoplatform solution as dispersing and stabilizing agent. After being further stirred for 12 h, the targeted CNMN was obtained. The content of ferric ions in the prepared CNMN was 8.6 μg/mg detected by an inductively coupled plasma mass spectrometer (ICP-MS; Perkin Elmer Optima 5300 DV).

Size distribution of CNMN was measured using a dynamic light scattering (DLS) (Brookhaven BI9000AT system, Brookheaven Instruments Co., USA) and transmission electron microscope (TEM, Hitachi H-7650, Japan).

T_1-T_2 MRI capability of CNMN evaluation

To measure the MRI ability of CNMN *in vitro*, the different concentrations of CNMN solution was added into 2.0 ml centrifuge tubes for the MRI test. The longitudinal (T_1) and transverse (T_2) relaxation rates were acquired on a clinic 7.0 T MR scanner (Bruker Corporation, 7.0 T, Germany). By linearly fitting the function of the inverse relaxation time to the metal ion concentration, the corresponding relaxation coefficients (r_1 and r_2) can be calculated.

For mice MRI studies, acquisition parameters were chosen as follows: flip angle=180, TR=498.3 ms, TE=14.0 ms, FOV=3×3, matrix=256×256, SI=1.0 mm/1.0 mm, averages=3, slices=16, NEX=1. Three tumor-bearing mice were selected randomly and anaesthetized using 100 ml chloral hydrate (4 %). 100 μl CNMN solution (0.25 mg/kg Fe) was injected by intratumoral or tail vein injection. MRI was performed at the desired time points after injection.

Measurement of photothermal performance

To evaluate the photothermal capability of CNMN nanoplatform solution *in vitro*, a series of different concentrations of CNMN (200 μl) were placed in a 96-well plate and then irradiated with the 808 nm NIR laser (1.6 W/cm^2) for 300 s. The temperature change was recorded every 10 s using a thermocouple probe. The CNMN solution was further imaged by a Fotric 220RD camera at 0 s, 30 s, 60 s, 120 s, 180s, 240s and 300s. To further test the photothermal stability of CNMN, sample of the CNMN (25 μg/ml of Fe concentration) was irradiated with NIR laser for 5 min (laser on), and then naturally cooled to room temperature (laser off). The cycles were repeated three times. The UV absorbance of CNMN solution was also detected after 12 cycles of laser on/off with 808 nm irradiation. .

The photothermal conversion efficiency (η) of CNMN solution was measured according to the method previous reported.[2] 1 ml CNMN aqueous dispersion (50 μg/ml of Fe concentration) was added into a quartz cuvette and irradiated with 808 nm NIR laser (1.6 W/cm^2) until the temperature was steady, then cooled naturally without laser. The value of η was calculated as the equation (1):

$$\eta = \frac{hs(T_{MAX} - T_{surr}) - Q_{dis}}{I(1 - 10^{-A_{808}})} \qquad (1)$$

where h is the heat transfer coefficient, s is the quartz cuvette surface area, T_{max} is the maximum temperature of the sample during laser irradiation (64 ℃), T_{min} is the room temperature (18 ℃), Q_{dis} is the energy consumed from light absorbe d by the quartz cuvette (0.23mW), I is the laser power (1.6 W/cm^2), and A_{808} is the absorbance of sample at 808 nm (1.085). The value of hs is calculated according to equation (2):

$$\tau_s = \frac{m_D c_D}{hs} \qquad (2)$$

Where τ_s is the sample system time constant (481.88 s); m_D and c_D are the mass (1.0 g) and heat capacity (4.2 J/g) of the deionized water, respectively. Therefore, hs was calculated to be 0.0087.

DOX loading and release behavior

DOX loading CNMN (DOX@CNMN) was fabricated by mixing 0.5 mg DOX with 10 mg CNMN at pH 7.4, with further stirring darkly for 24 h at room temperature. Unloaded DOX was removed by centrifugation. The DOX content in DOX@CNMN was detected by fluorescence spectrophotometer (EX: 488 nm, EM: 555 nm) after acidification and the calculated DOX loading efficiency was 7.89% W/W.

The DOX and ferric ions release from DOX@CNMN was performed by dialysis against different pH buffers (pH 5.0, 6.8 and 7.4). The dialysis bag containing 1 ml of DOX@CNMN aqueous dispersion was immersed in 40 ml release medium and stirred at 100 rpm at 37.0 ± 0.5 °C. At predetermined intervals, 1 ml sample was collected and the concentration of DOX and ferric ions was measured by fluorescence spectrophotometer and ICP-MS, respectively.

Cell culture and animal experiments

Murine breast cancer cells (4T1), rat myocardial cells (H9c2) and human proximal renal tubule epithelial cells (HK-2) were all obtained from the American Type Culture Collection

(ATCC). 4T1 and H9c2 cells were cultured in DMEM and HK2 cells were cultured in DMEM-F12 supplemented with 10% FBS and 1% penicillin/streptomycin.

All animal study protocols were designed according to the guiding principle set by the National Institutes of Health Guide for the Care and Use of Laboratory Animal. For the tumor model, each Balb/c female mice was subcutaneously injected with 100 μl PBS containing 5×10^6 4T1 cells at the mammary fat pad. Animal studies were performed until the solid tumors reached 50 to 100 mm^3.

***In vitro* antitumor efficacy evaluation**

To evaluate the chemo-photothermal therapeutic capability of DOX@CNMN, 4T1 cells were respectively incubated with CNMN and DOX@CNMN (at the DOX concentration of 1.25 μg/ml and the Fe content of 12.5 μg/ml) for 4 h. For the laser groups, the cells were exposed to the 808 nm NIR for 300 s and further incubated for 20 h. The 4T1 cell viabilities were determined using MTT assay and Annexin V-FITC/PI apoptosis detection kit simultaneously.

Cellular uptake of DOX@CNMN

Flow cytometry (FCM) and confocal laser scanning microscopy (CLSM) were carried out simultaneously to explore the cellular uptake behavior of DOX@CNMN. For FCM, the 4T1 cells were cultured in a 6-well plate and incubated with DOX@CNMN and free DOX (the DOX concentration was 2.5 μg/ml) for 2 h and 4 h, respectively. The intracellular DOX content of different groups was detected by FCM, and the corresponding Fe content was determined by ICP-MS.

For CLSM, 4T1 cells were cultured in the confocal dishes and incubated with DOX@CNMN and free DOX (the DOX concentration was 2.5μg/ml) for 2 h and 4h respectively. The cells were then stained with DAPI for 10 min. Finally, the cells were washed with PBS for three times and imaged by CLSM (Leica TCS SP5, Germany).

***In vivo* distribution**

To observe and estimate the tumor-targeted efficacy of CNMN, Cy7-loaded CNMN (Cy7@CNMN) was prepared through mixing 0.1mg Cy7 with 10mg CNMN solution at pH 7.4. Six 4T1 tumor-bearing mice were administered with 1 mg kg^{-1} (Cy7 dose) of Cy7@CNMN intravenously and imaged at 6, 12, 24 and 36 h post-injection using a bio-imaging system (VIEWORKS, Korea) at excitation wavelength of 720 nm and emission of 790 nm.

4T1 tumor-bearing mice were randomly divided into two groups with twelve animals in each group. Each mouse was administered free DOX or DOX@CNMN at 5mg/kg DOX dose through tail vein injection, and then sacrificed at preset time points. The main organs (heart, liver, spleen, lung and kidney) and tumors were collected, weighed and homogenized. The content of DOX was detected by fluorescence spectrophotometer at excitation wavelength of 488nm and emission of 555nm.

***In vivo* photothermal activity evaluation**

Six mice were divided into two groups averagely and administrated with 100 ul PBS or DOX@CNMN solution (at Fe content of 0.5 mg kg^{-1}) via tail vein injection. The tumor was irradiated with 808 nm laser (1.6W/cm^2) for 240 s at 24 h post-injection. The tumor temperature was recorded r imaged by Fotric 220RD camera at 0 s, 30 s, 60 s, 120 s, 180s and 240s.

***In vivo* anti-tumor efficiency and biosafety evaluation**

Mice bearing 4T1 tumors were divided into six groups randomly (five mice per group) and treated with (i) Saline, (ii) CNMN + NIR laser, (iii) CNMN, (iv) Free DOX, (v) DOX@CNMN and (vi) DOX@CNMN + NIR laser via tail vein injection (2.5 mg/kg DOX and 0.5mg/kg Fe). The first day of dosing was designated as day 0. The tumors were irradiated by 808 nm laser (1.6 W/cm^2) for 4 min at 24 h post-injection. Treatment administrations and laser irradiation were repeated on days 2 and 3. Tumor sizes and body weights of mice were recorded every other day. Tumor volume (V) was calculated as $V = d^2 \times D/_2$, where D and d is the longest

and shortest diameter of the tumor, respectively.[3] At day 14, the mice were sacrificed. The tumors was harvested, weighted and stained with H&E.

Biosafety analysis

In vivo safety evaluation of CNMN was performed on healthy mice. The mice were divided into two groups randomly (Five mice per group) and then injected with 100 μl Saline or CNMN (Fe^{3+} was 0.5mg/kg) intravenously. After several weeks, the blood of different group mice was also collected for routine tests. The major organs including heart, liver, spleen, lungs, and kidneys were harvested for H&E staining.

Statistical analysis

The experimental data was presented as mean ± standard deviation (SD). The comparison between different groups was characterized using Student's t-test and considered to be statistically significant when the value reached $*p < 0.05$, $**p < 0.01$, $***p < 0.001$.

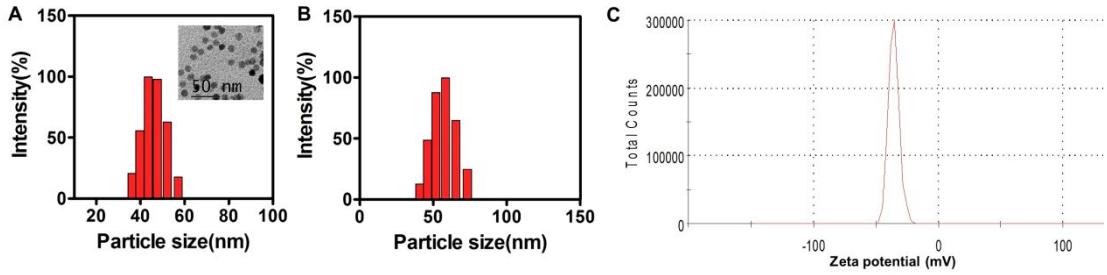

Figure S1 Size distribution of (A) γ-Fe_2O_3, and (B) Fe_2O_3@PDA. (C) The zeta potential of CNMN

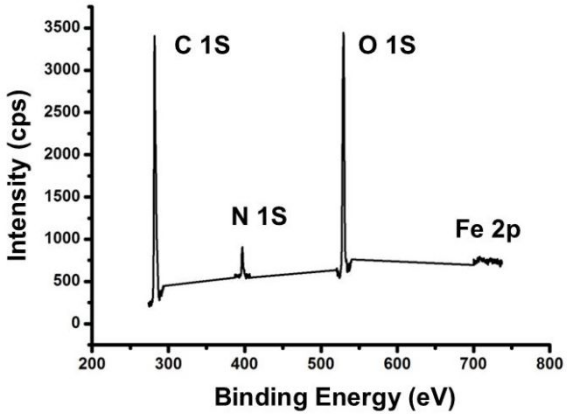

Figure S2 XPS analysis of CNMN

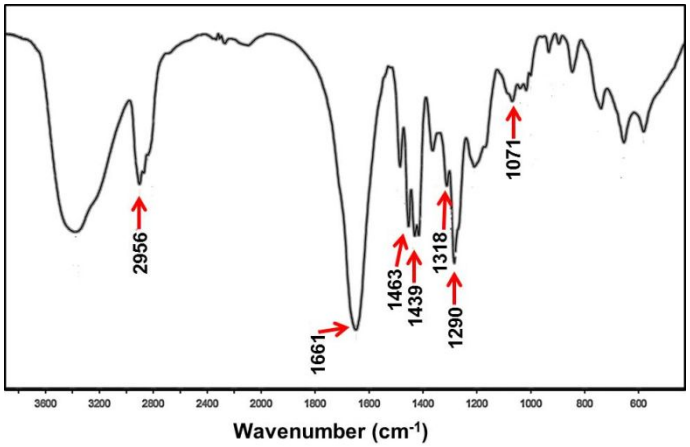

Figure S3 FTIR spectrum of CNMN.

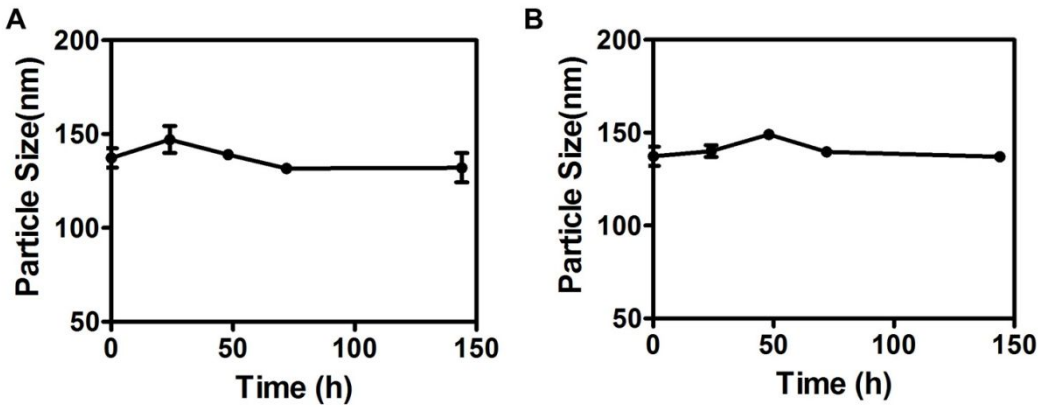

Figure S4 Real-time changes in the diameter of CNMN under pH 7.4 PBS solution and RPMI 1640 medium. (n=3)

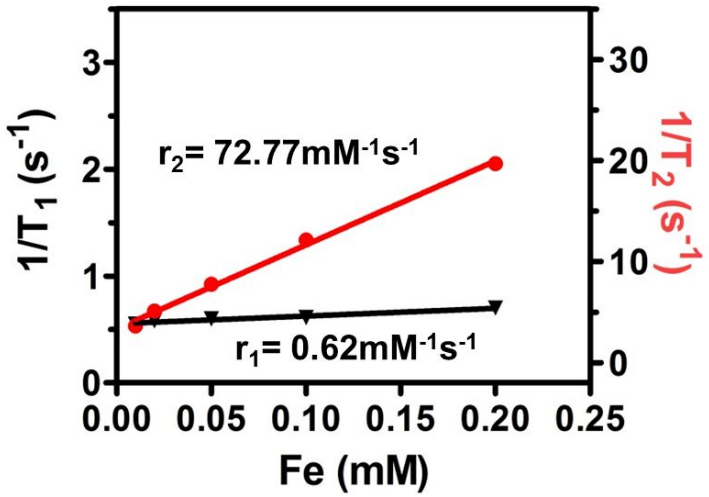

Figure S5.r_1 and r_2 value of original Fe_2O_3 as a function of the molar concentration of Fe^{3+} in the solution.

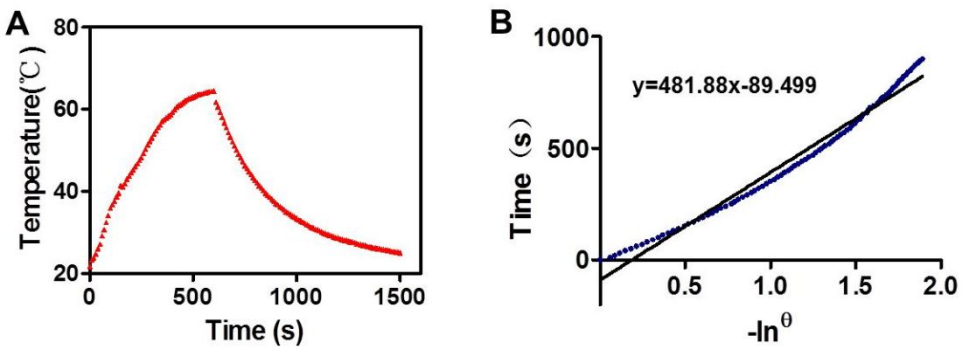

Figure S6 (A) Photothermal effect of the CNMN aqueous solution (at Fe content of 50 μg/ml) with the 808 nm laser (1.6 W/cm^2). (B) Plot of cooling time versus negative natural logarithm of the temperature driving force obtained from the cooling stage as shown in (A). The time constant for heat transfer of the system is determined to be τ_s = 481.88 s

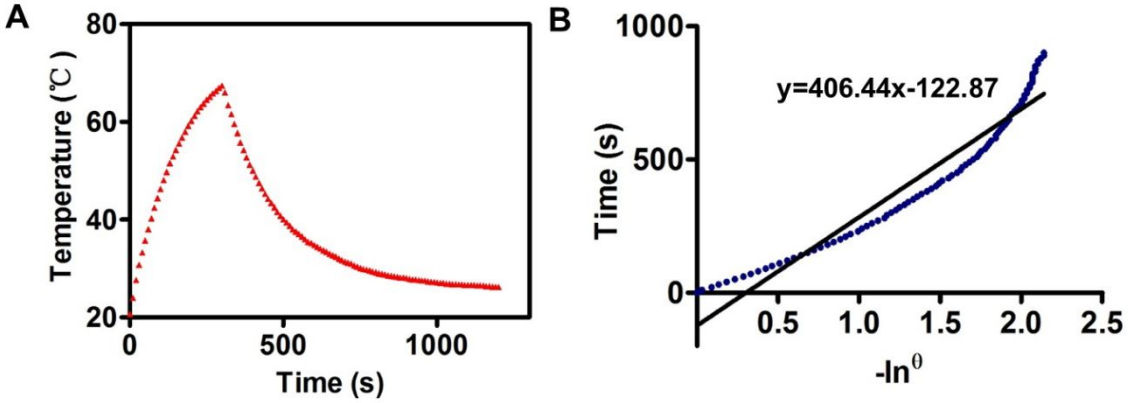

Figure S7 (A) Photothermal effect of the CNMN aqueous solution when illuminated with the 808nm laser (1.6 W/cm^2) at pH 5.0. (B) Plot of cooling time versus negative natural logarithm of the temperature driving force obtained from the cooling stage as shown in (A). The time constant for heat transfer of the system is determined to be τs = 406.44 s. The the photothermal conversation efficiency of CNMN at pH 5.0 was calculated to be 26.5 %.

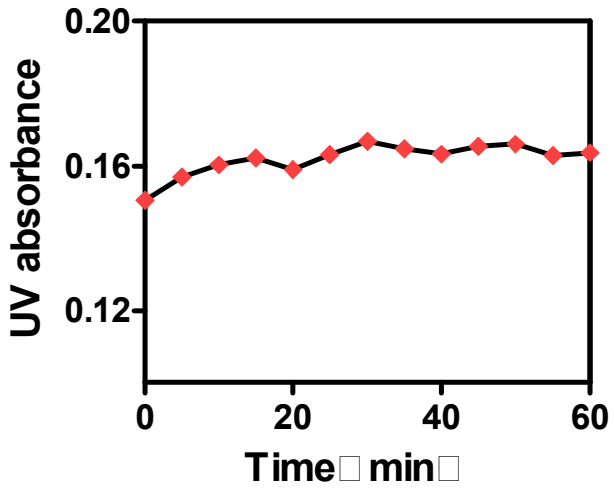

Figure S8 The absorbance of CNMN at 808 nm as a function of laser irradiation time.

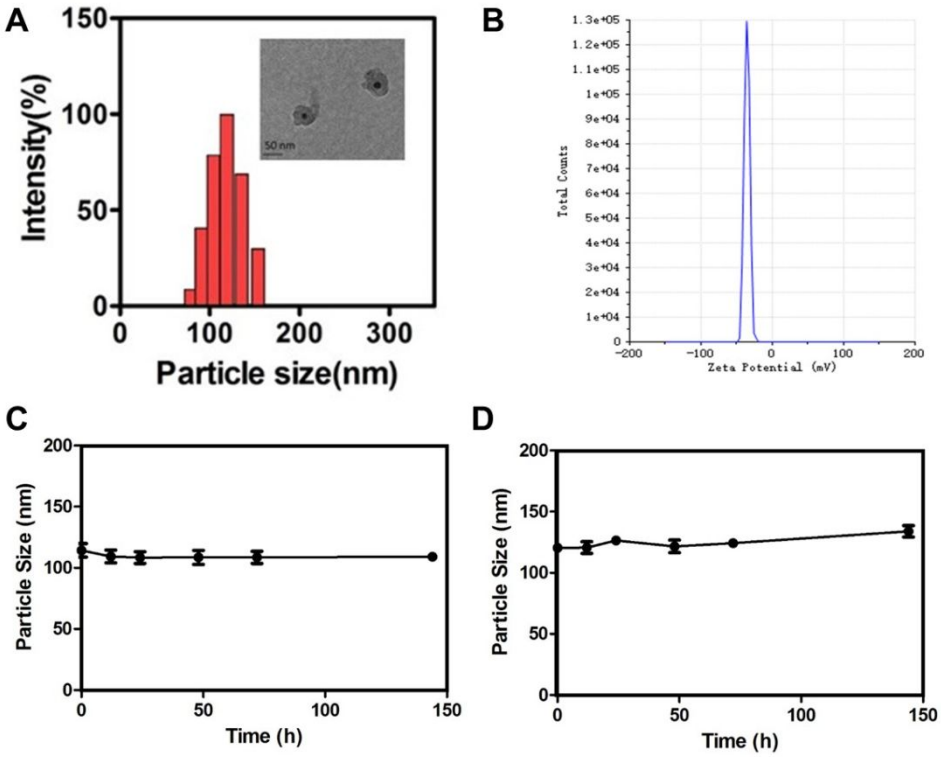

Figure S9 (A) Size distribution of DOX@CNMN detected by DLS. (B) The zeta potential of DOX@CNMN. (C/D) Real-time changes in the diameter of DOX@CNMN under pH 7.4 PBS solution (C) and RPMI 1640 medium (D). (n=3)

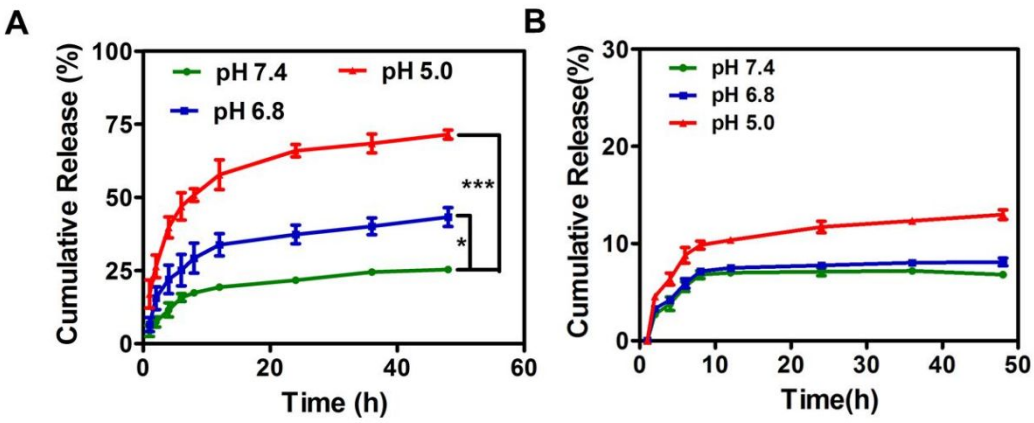

Figure S10 (A) DOX and Fe release profile over time at different pH conditions. (n=3) *p < 0.05, ***p < 0.001.

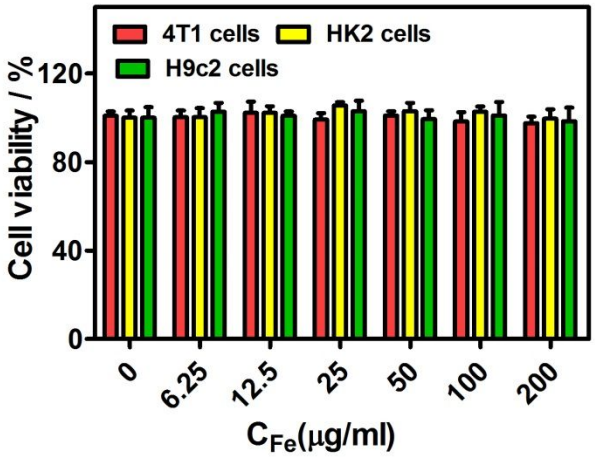

Figure S11 In vitro cytotoxicity of CNMN against 4T1, HK2 and H9c2 cells respectively after 24 h incubation (n =3).

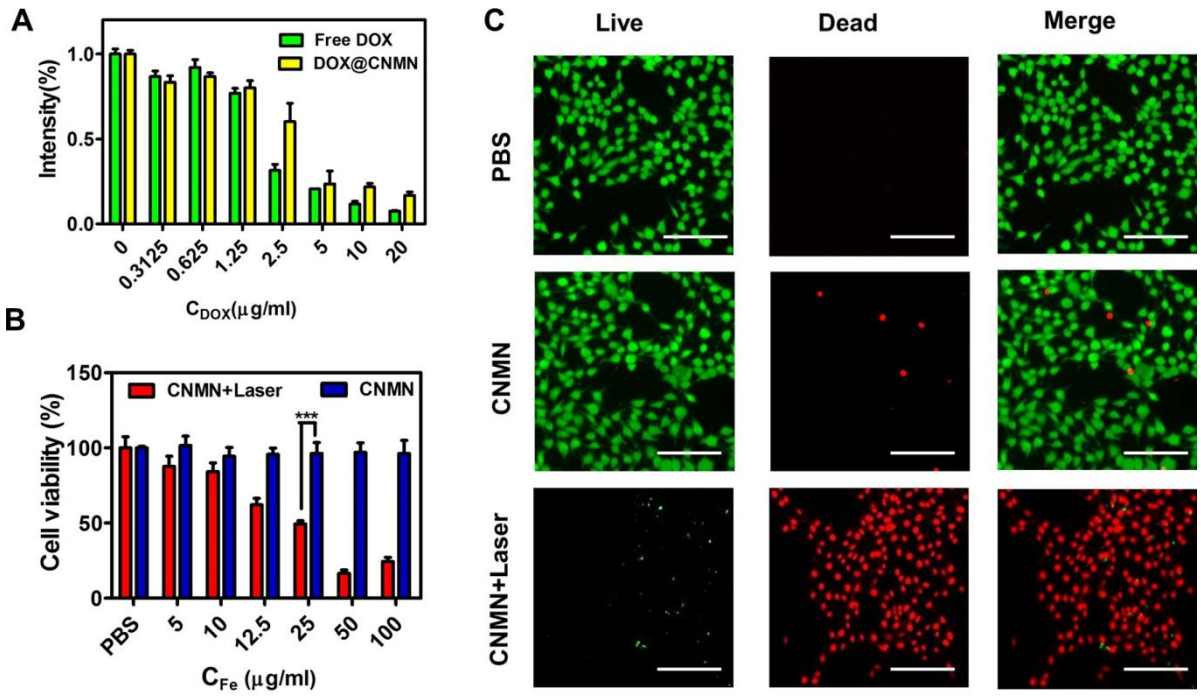

Figure S12 (A) In vitro cytotoxicity of free DOX and DOX@CNMN against 4T1 cells after 24 h incubation (n =3). (B) The viabilities of 4T1 cell after incubating with different concentrations of CNMN with or without laser (n=3). (C) Photographs of 4T1 cells stained with Calcein-AM (green, live cells) and PI (red, dead cells) imaged using a fluorescence microscope after incubation with CNMN (Fe content: 25 μg/ml) under 808 nm NIR laser irradiation for 300 s. Scale bar is 100 μm.

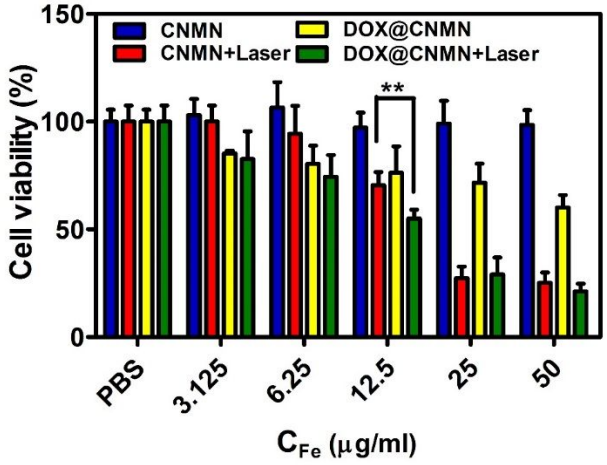

Figure S13 The viabilities of 4T1 cell after incubating with different concentrations of CNMN and DOX@CNMN with or without 808 nm laser irradiation (n=3).

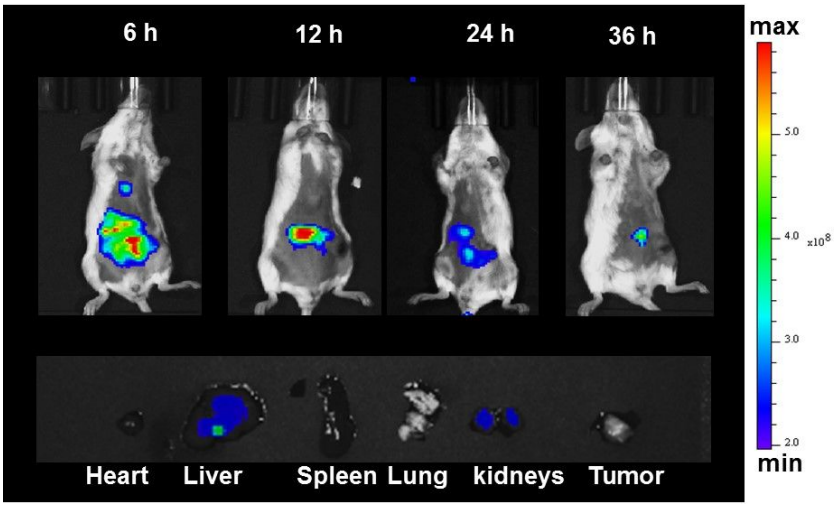

Figure S14 Fluorescence images of mice injected by free Cy7 (1 mg/kg) at different time, and the images of isolated tumor and major organs at 36 h post-injection.

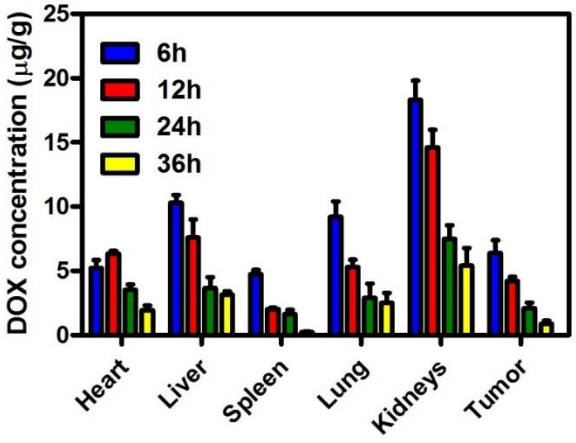

Figure S15 Quantitative analysis for DOX tumor accumulation in 4T1 tumor-bearing mice at different time intervals after i.v. of free DOX (n=3).

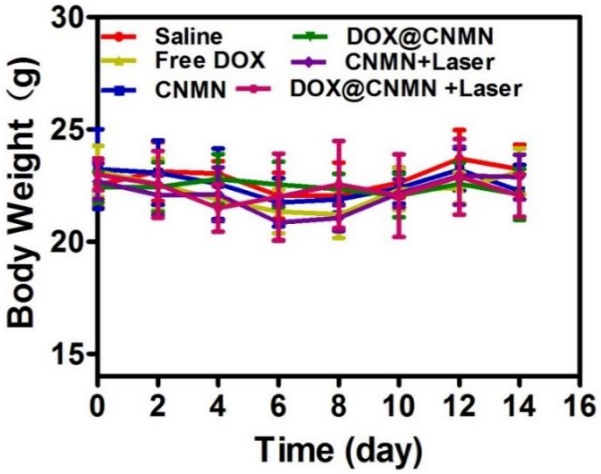

Figure S16 Body weight profiles of the different groups. (n=5)

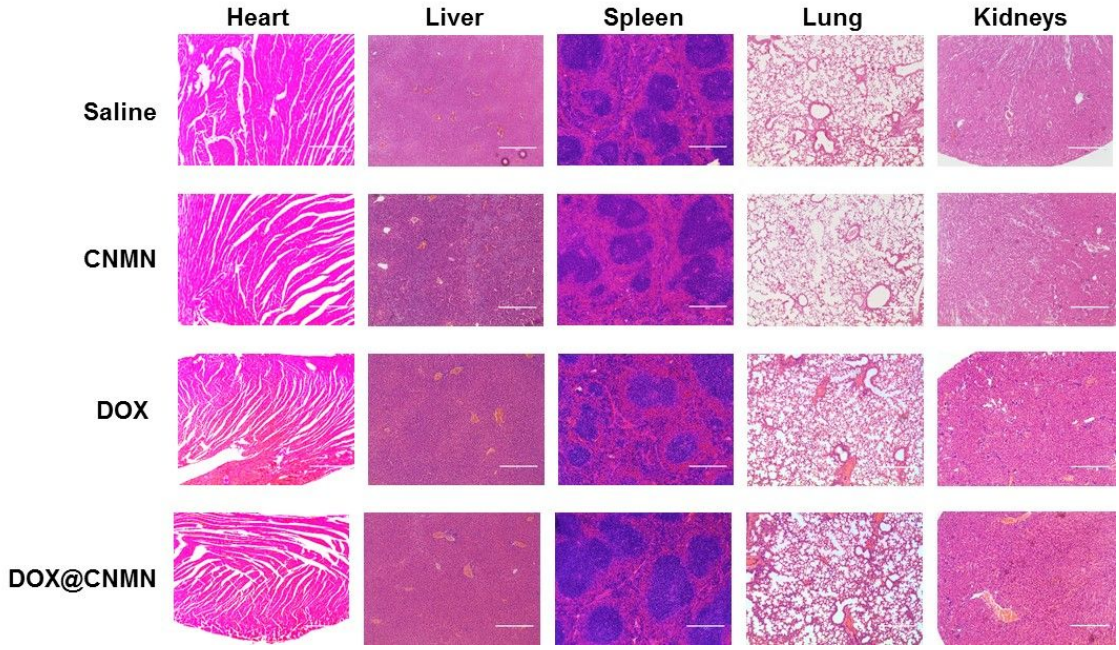

Figure S17 H&E staining images of major organs (heart, liver, spleen, lung, kidneys) in the group injected with tested dose of different groups on the healthy mice. The scale bar is 400 μm.

Table S1 Hematological parameters after i.v. injections. Data are shown as mean ± SD (n = 3).

	WBC (10^9/L)	Gran (10^9/L)	RBC (10^{12}/L)	HGB (g/L)	Platelet (10^9/L)	RDW (%)
Saline	4.78±0.67	1.23±0.24	7.56±1.31	125±13	1108±78	15.65±0.44
CNMN	5.06±0.18	1.13±0.18	8.09±1.02	135±11	824±245	14.12±0.13
DOX	4.42±0.23	0.98±0.16	8.18±1.19	122±12	765±117	14.87±0.24
DOX@CNMN	5.86±0.39	1.21±0.22	7.98±0.89	119±17	879±166	13.59±0.38

Table S2. The parameters of liver and renal functions in healthy mice after tail vein injection. Data are shown as mean ± SD (n = 3).

	Liver functions			Renal functions	
	AST (U/L)	ALT (U/L)	ALP (U/L)	BUN (mg/dL)	CR (uM)
Saline	110.3±8.2	88.5±6.9	261.1±17.6	21.8±2.2	35.6±4.7
DOX@CNMN	198.7±11.4	127.6±5.6	319.6±10.4	24.6±3.8	32.5±5.6
Reference	67~381	40~170	108~367	7~31	17.68~44.2

References

1. Chen, C. J.; Wang, J. C.; Zhao, E. Y.; Gao, L. Y.; Feng, Q.; Liu, X. Y.; Zhao, Z. X.; Ma, X. F.; Hou, W. J.; Zhang, L. R.; Lu, W. L.; Zhang, Q., Self-assembly cationic nanoparticles based on cholesterol-grafted bioreducible poly(amidoamine) for siRNA delivery. *Biomaterials* **2013,** *34* (21), 5303-5316.
2. Lv, G.; Guo, W.; Zhang, W.; Zhang, T.; Li, S.; Chen, S.; Eltahan, A. S.; Wang, D.; Wang, Y.; Zhang, J.; Wang, P. C.; Chang, J.; Liang, X. J., Near-Infrared Emission CuInS/ZnS Quantum Dots: All-in-One Theranostic Nanomedicines with Intrinsic Fluorescence/Photoacoustic Imaging for Tumor Phototherapy. *ACS nano* **2016**.
3. Li, H.; Yang, X.; Zhou, Z.; Wang, K.; Li, C.; Qiao, H.; Oupicky, D.; Sun, M., Near-infrared light-triggered drug release from a multiple lipid carrier complex using an all-in-one strategy. *Journal of controlled release : official journal of the Controlled Release Society* **2017,** *261*, 126-137.